

A design of a nanometer size metal particle generator: Thermal decomposition of metal carbonyls

S. H. Huh, S. J. Oh, Y. N. Kim, and G. H. Lee^{a)}

Department of Chemistry, College of Natural Sciences, Kyungpook National University, Taegu 702-701, South Korea

(Received 14 January 1999; accepted for publication 9 August 1999)

We have developed a method which can produce both pure and alloy nanometer size metal particles in a large scale. This method combines a thermal decomposition of metal carbonyls with a collision induced clustering. Metal carbonyls are thermally decomposed with a hot filament and resultant bare metal atoms undergo collisions to produce nanometer size metal particles. This method requires a very simple experimental setup even though it is a high efficiency production method. Using this method, we have produced, high purity Fe, Mo, and alloy Fe/Mo nanometer size metal particles.

© 1999 American Institute of Physics. [S0034-6748(99)03111-1]

I. INTRODUCTION

Nanometer size metal particles (or clusters) are now emerging as new materials because of their potential industrial applicabilities to a variety of areas.¹ Thus studies on nanoparticles are rapidly expanding.¹⁻²⁴ They possess unique mechanical, physical, and chemical properties different from their corresponding bulk. Using such properties, they can be used as electrical materials, magnetic materials, superconductors, nonlinear optical materials, and catalysts, etc. Some of these properties are size dependent.^{1,21,22} Such size dependence allows us to design a variety of *state of art* nanostructured devices such as light emitting diodes and lasers, etc.²³

For instance, Fe nanometer size metal particles possess magnetic property²⁴ and thus are now used as a magnetic coating material in a magnetic tape or in memory devices. They also strongly absorb ultraviolet (UV) photons in a wide range (200–600 nm) and thus can be used as an efficient UV protector in cosmetics.²⁵ Fe₂O₃ nanoparticles tint red brown and thus can be used as pigment as well as an UV protector because they also strongly absorb UV photons in a wide range.²⁶

A large scale production of high purity nanoparticles at a low cost is essential for industrial usages. Besides these, particle size control is also important because a different size provides a different property. Size control can be achieved by carefully changing metal vapor density;^{2,5,8} in the present method, metal vapor density is controlled by changing metal carbonyl vapor density because metal atoms are supplied by decomposition of metal carbonyl vapors.

Here, we designed a nanometer size metal particle generator (NMSMPG) which can produce a variety of both pure and alloy nanometer size metal particles in a high purity, at a low cost, and in a large scale. This method is very simple compared to laser ablation^{8,9} and sputtering methods.⁵⁻⁷ In this article we produced pure Fe and Mo nanoparticles as

well as alloy Fe/Mo nanoparticles and characterized their size and structure.

II. EXPERIMENTAL SETUP

The NMSMPG which is used to produce nanometer size metal particles is presented in Fig. 1. It consists of two main parts which are the reaction chamber and the filament.

The reaction chamber is made of stainless steel (SUS 304). The reaction chamber is a pipe type with a dimension of the out diameter = 50 mm × the length (L) = 100 mm and was evacuated with a 150 ℓ/s mechanical pump down to 10^{-3} Torr. Even at this vacuum level, oxides production was minimal. The 3 in. top flange with two filament feedthroughs is copper gasket sealed. Two $\frac{1}{4}$ in. stainless steel tubes welded to the middle of the reaction chamber are for evacuation of gases and introduction of sample vapors, respectively (see Fig. 1). The gas handling cart, which is equipped with an 150 ℓ/s mechanical pump and vacuum gauges, was used to introduce gases and to evacuate the reaction chamber.

The filament connected to the top flange electrical feedthroughs is a resistive heater. The gap between two electrical feedthroughs was 1 cm apart. When the distance between the two feedthroughs was short, metal particles sometimes caused an electrical shortage. In order to increase the area for thermal decomposition reaction, a solenoid shape filament was used as shown in Fig. 1. Length was 80 mm but it could be changed. A 1-mm-thick nichrome (Ni/Cr/Fe alloy) wire with a total resistance of 2.3 Ω was used in this experiment. However, any kind of resistive material can be used. The filament was heated by flowing current (alternating current in this experiment) through it.²⁷

A separate sample container was attached to the reaction chamber with a swagelok valve between them. In this configuration, metal carbonyl vapor was provided continuously to the reaction chamber while decomposition reaction was occurring. The reaction chamber sometimes needs being evacuated to reduce its pressure because of pressure rise due to COs from decomposition of metal carbonyl vapors.

^{a)}Author to whom correspondence should be addressed; electronic mail: ghlee@bh.kyungpook.ac.kr

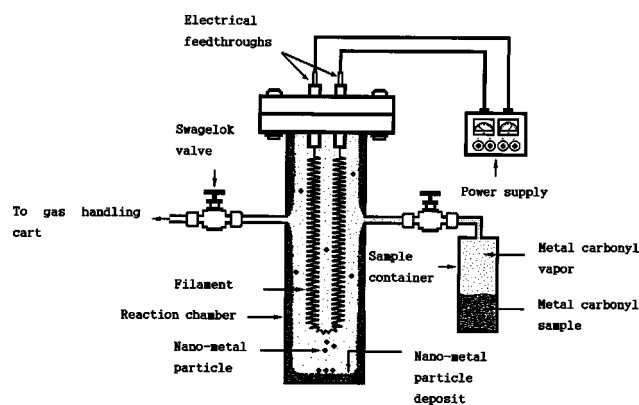


FIG. 1. A schematic experimental set up of the NMSMPG.

Sample container was slightly heated up to 50–60 °C except for $\text{Fe}(\text{CO})_5$ because $\text{Fe}(\text{CO})_5$ has 20–30 Torr vapor pressure at room temperature. Reaction chamber should be maintained a few degree higher than the sample container to avoid recrystallization of metal carbonyl vapors which might decrease a purity of metal particles. The radiatively heated reaction chamber temperature by the filament was 60–70 °C because the present chamber was small. Thus, a separate heating was not necessary. However, when a larger reaction chamber is used as described later, a separate heating will be needed.

The experimental setup presented in Fig. 1 can be modified into a larger size to increase production rate. It is recommended to use several filaments at different locations when a larger reaction chamber is used. This allows us to produce metal particles in a short time and to continue decomposition reaction even when one of the filaments fails due to such as an electrical shortage.

A glass chamber which has a similar dimension as the stainless steel chamber was also made and used. However, there was no difference in performance. Metal particles forming near to the filament environment as well as the filament color were easily observed using the glass reaction chamber.

III. RESULTS AND DISCUSSION

A. Production condition

Metal carbonyl samples, $\text{Fe}(\text{CO})_5$ and $\text{Mo}(\text{CO})_6$, were used. We can change two conditions which are (1) the metal carbonyl vapor pressure and (2) the filament voltage.

In general, we found that high purity metal particles could be steadily produced at mild conditions which correspond to 10–30 Torr of metal carbonyl vapor pressure and a slightly glowing filament voltage [17 VAC for $\text{Fe}(\text{CO})_5$ and 25 VAC for $\text{Mo}(\text{CO})_6$ were used in this experiment].²⁷ At these conditions, high purity metal particles were uniformly deposited on the reaction chamber wall.

We noticed that oxides were produced at high filament voltages. We think that the oxide product came from reaction with oxygen of COs decomposed by a hot filament and with some residual O_2 in the reaction chamber at high filament voltages. However, we usually obtained purities of >95% and >98% for Fe and Mo particles, respectively, at mild

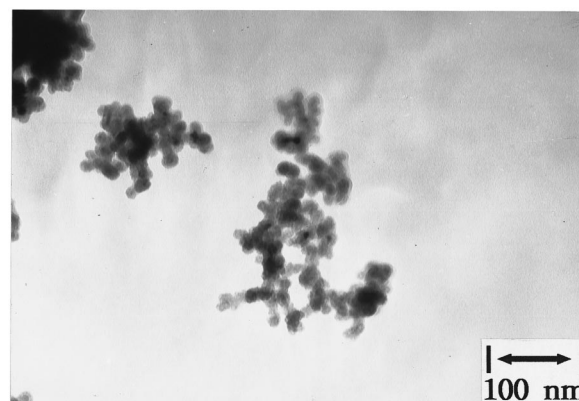


FIG. 2. A low resolution TEM of Fe particles. Particle size is homogeneous with a size distribution between 5.0 and 7.0 nm.

conditions described earlier. The purity even increased by using a lower filament voltage. We also noticed that metal particles collected on the filament contained some oxides and thus were not collected.

Although a high metal carbonyl vapor pressure (>1 atm) is not normally used in the experiment, it should not be run at high filament voltages because of a possibility of explosion originating from a rapid pressure rise. Note that decomposition of metal carbonyl [$\text{M}(\text{CO})_x$] produces x times the initial metal carbonyl vapor pressure. Since we used a metal carbonyl vapor pressure usually less than 50 Torr, the explosion never happened. In the case of the $\text{Fe}(\text{CO})_5$ sample, thread-like products were produced near to the filament environment at a high filament voltage. Thus, in general, a high filament voltage should not be used.

B. Yields and costs

When 1 g of $\text{Fe}(\text{CO})_5$ was used, we obtained 250 ± 50 mg of Fe particles; a theoretical yield is 286 mg. Each run took 5–10 min. The loss was mainly due to uncollected particles from the reaction chamber. Costs needed for production are mostly those of metal carbonyl samples because the experimental setup is very simple. Using 1 kg of $\text{Fe}(\text{CO})_5$, which costs 112.35 US dollars will produce ~250 g of Fe particles, which indicates a production cost of 45 cents/g.

C. Particle size and structure

Final product, i.e., metal particles always tinted black. Three experimental results are presented here. They are (1) pure Fe nanoparticles, (2) pure Mo nanoparticles, and (3) alloy Fe/Mo nanoparticles.

Figure 2 represents a low resolution transmission electron micrograph (TEM) of Fe particles. Figure 3 represents an x-ray diffraction (XRD) pattern of Fe particles which shows a body-centered-cubic (bcc) structure. Note that the bulk Fe also possesses a bcc structure. Particle size is very homogeneous with an average particle diameter of 6.0 nm.

Both Figs. 4(a) and 4(b) represent low resolution TEMs of Mo particles, respectively. Figure 5 represents an XRD pattern of Mo particles which shows a face-centered-cubic (fcc) structure. However, the bulk Mo possesses a bcc structure. This structural difference is due to the fact that a small

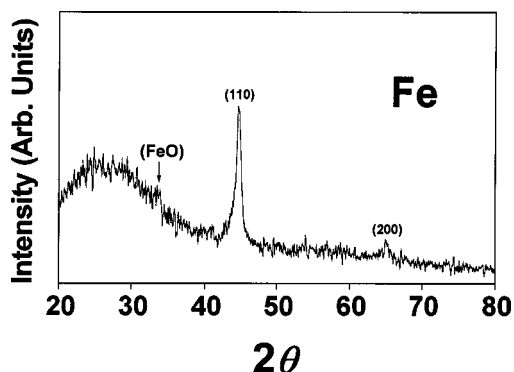


FIG. 3. An XRD pattern of Fe particles. The assignment is miller indices (hkl). Structure is bcc.

particle can have a structure different from the bulk. Such a structural difference had also been observed in metal particles produced by a CO_2 laser multiphoton decomposition method of metal carbonyls by our group.⁴ This result is also consistent with a theoretical prediction by Tománek, Mukherjee, and Bennemann.²⁸ There exist two kinds of particle size; one is small particles with a homogeneous size distribution between 2.0 and 3.0 nm and the other is large

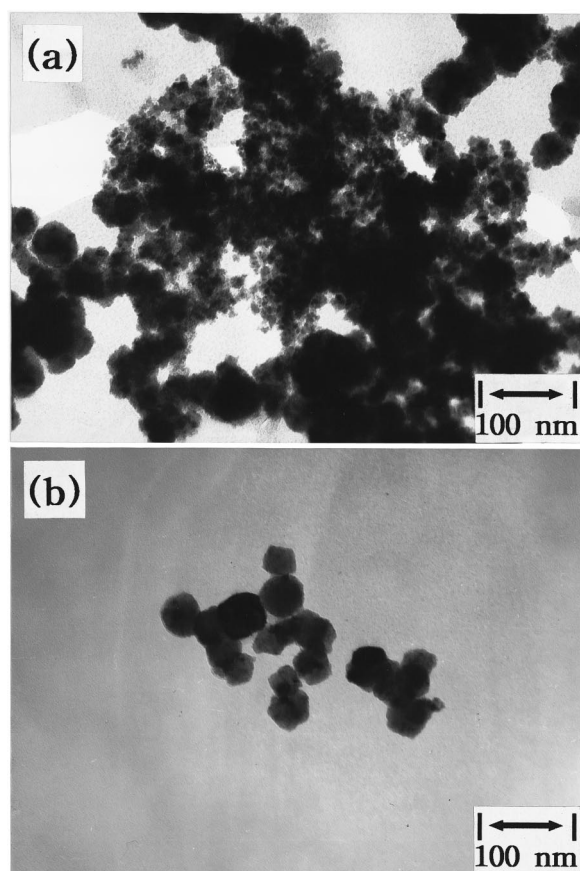


FIG. 4. Low resolution TEM of Mo particles. (a) Both small and large particles are shown. (b) Only large particles are shown. Two kinds of particle size exist; one is small particles with a homogeneous size distribution between 2.0 and 3.0 nm and the other is large particles with a somewhat wide size distribution between 30.0 and 50.0 nm. A close examination of large particles shows that they are nearly square in shape. Square shape of Mo particles had been observed in the argon ion sputtering experiment (see Refs. 5–7).

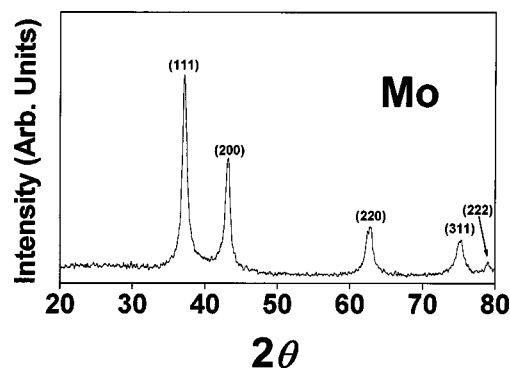


FIG. 5. An XRD pattern of Mo particles. The assignment is miller indices (hkl). Structure is fcc. Note that the bulk has bcc structure. This structural difference is due to a particle size effect (see Ref. 4).

particles with somewhat a wide size distribution between 30.0 and 50.0 nm. Since the XRD pattern shows only a fcc structure, it seems that the large particles are aggregates (probably due to self arrangement) of the small particles. Note that a self-arrangement had been observed in Mo particles produced by the argon ion sputtering method.^{5–7} Figure 4(b) shows that some of the large particles are nearly square, which had been also observed in Mo particles produced by the argon ion sputtering method.^{5–7}

Alloy nanometal particles with a variety of composition can be produced by using several metal carbonyl samples and by changing the ratio in amount of metal carbonyl samples.²⁹ Figure 6(a) represents an XRD pattern of $\text{Fe}_{68}\text{Mo}_{32}$ alloy nanoparticles by mole percent from elemental analysis which were produced using ~ 10 Torr $\text{Fe}(\text{CO})_5/\sim 5$ Torr $\text{Mo}(\text{CO})_6$ and Fig. 6(b) represents an XRD pattern of a physical mixture of 68% Fe and 32% Mo nanoparticles by mole percent. As expected, the physical mixture [Fig. 6(b)] shows a combination of the XRD patterns of pure Fe and pure Mo nanoparticles, as presented in Figs. 3 and 5,

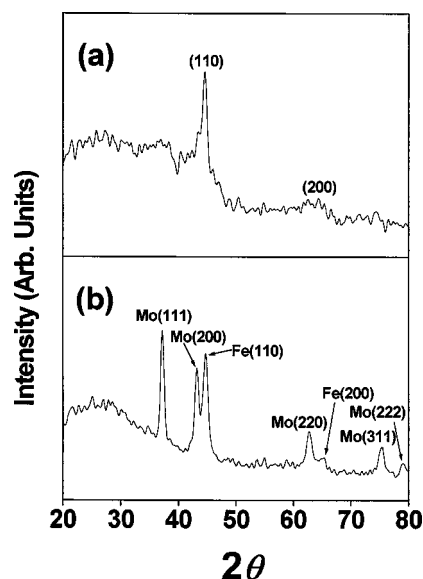


FIG. 6. (a) An XRD pattern of alloy $\text{Fe}_{68}\text{Mo}_{32}$ particles by mole percent. (b) An XRD pattern of a physical mixture of 68% Fe and 32% Mo particles by mole percent. The assignment is miller indices (hkl). Two XRD patterns are provided to distinguish the alloy particles from the physical mixture.

respectively. However, Fig. 6(a) shows only one bcc structure. We think that the bcc structure of alloy particles resulted from the bcc Fe nanocrystal into which Mo atoms were homogeneously embedded. However, inhomogeneous alloy may show both fcc and bcc structures in the XRD pattern (because a Mo rich nanocrystal will show fcc structure whereas an Fe rich nanocrystal will show a bcc structure and thus both fcc and bcc structures will appear in the XRD pattern). However, the inhomogeneous alloy is still distinguishable from the physical mixture because the XRD peak intensities are different from each other.²⁹

ACKNOWLEDGMENT

The authors gratefully acknowledge the supports of the '98 Kyungpook National University research fund. The authors thank KBSI for allowing us to use the TEM, XRD, and Inductively coupled plasma-atomic emission spectrometer at a membership rate.

¹R. W. Siegel, *Phys. Today* **46**, 64 (1993).

²C. G. Granqvist and R. A. Buhrman, *J. Appl. Phys.* **47**, 2200 (1976).

³C. Hayashi, *J. Vac. Sci. Technol. A* **5**, 1375 (1987).

⁴G. H. Lee, S. H. Huh, and H. I. Jung, *J. Mol. Struct.* **440**, 141 (1998).

⁵A. S. Edelstein, G. M. Chow, E. I. Altman, R. J. Colton, and D. M. Hwang, *Science* **251**, 1590 (1991).

⁶G. M. Chow, C. L. Chien, and A. S. Edelstein, *J. Mater. Res.* **6**, 8 (1991).

⁷G. M. Chow, R. L. Holtz, A. Pattnaik, A. S. Edelstein, T. E. Schlesinger, and R. C. Cammarata, *Appl. Phys. Lett.* **56**, 1853 (1990).

⁸M. S. El-Shall, D. Graiver, U. Pernisz, and M. I. Baraton, *Nanostruct. Mater.* **6**, 297 (1995).

⁹B. J. Jönsson, T. Turkki, V. Störm, M. S. El-Shall, and K. V. Rao, *J. Appl. Phys.* **79**, 5063 (1996).

¹⁰M. S. Nashner, A. I. Frenkel, D. L. Adler, J. R. Shapley, and R. G. Nuzzo, *J. Am. Chem. Soc.* **119**, 7760 (1997).

¹¹K. S. Suslick, T. Hyeon, and M. Fang, *Chem. Mater.* **8**, 2172 (1996).

¹²T. G. Nieh, P. Luo, W. Nellis, D. Lesuer, and D. Benson, *Acta Mater.* **44**, 3781 (1996).

¹³M. Z.-C. Hu, M. T. Harris, and C. H. Byers, *J. Colloid Interface Sci.* **198**, 87 (1998).

¹⁴D. A. Bonnell, Y. Liang, M. Wagner, D. Carroll, and M. Rühle, *Acta Mater.* **46**, 2263 (1998).

¹⁵S. L. Girshick, N. P. Rao, and M. Kelkar, *J. Vac. Sci. Technol. A* **14**, 529 (1996).

¹⁶M. Bohenek, A. S. Myerson, and W. M. Sun, *J. Cryst. Growth* **179**, 213 (1997).

¹⁷G. R. Odette and B. D. Wirth, *J. Nucl. Mater.* **251**, 157 (1997).

¹⁸M. J. Uttormark and J. H. Perepezko, *J. Non-Cryst. Solids* **205–207**, 550 (1996).

¹⁹K. R. Roos and M. C. Tringides, *Surf. Sci.* **355**, L259 (1996).

²⁰J. D. Franolic, J. R. Long, and R. H. Holm, *J. Am. Chem. Soc.* **117**, 8139 (1995).

²¹M. L. Steigerwald *et al.*, *J. Am. Chem. Soc.* **110**, 3046 (1988).

²²Ph. Buffat and J.-P. Borel, *Phys. Rev. A* **13**, 2287 (1976).

²³For example, see the special issue on optics of nanostructures, *Phys. Today* **46**, 22 (1993).

²⁴L. Del Bianco, C. Ballesteros, J. M. Rojo, and A. Hernando, *Phys. Rev. Lett.* **81**, 4500 (1998).

²⁵We recorded UV absorption spectrum of Fe nanoparticles which strongly absorbed UV between 200–600 nm.

²⁶We produced Fe₂O₃ nanoparticles by heating Fe nanoparticles up to 400 °C while flowing O₂ with a flowing speed of 100 ml/min. They tinted red brown and strongly absorbed UV between 200–600 nm.

²⁷Technical data from Pelican Wire Company Inc., Naples, FL 34109-1896. The filament used in this experiment (1 mm thick, 2.3 Ω, and nichrome wire [Ni/Cr/Fe alloy]) provides 380 °C filament temperature at 17–24 VAC filament voltages according to the technical data.

²⁸D. Tománek, S. Mukherjee, and K. H. Bennemann, *Phys. Rev. B* **28**, 665 (1983).

²⁹S. H. Huh, S. J. Oh, Y. N. Kim, H. K. Kim, J. W. Park, and G. H. Lee (unpublished).